Table II. Corrected Efficiencies of Benzil-Sensitized Photoepoxidations (0.1 M Solutions in Benzene, 5 °C)

olefin	*t*, h	% epoxide	% benzil recovered	epoxide/ benzil consumed	ref
$Ph_2C{=}CMe_2$	0.25	80	42	1.4	2
PhCH=CHMe					
trans	0.25	96	48	1.8	2
cis	0.25	89	45	1.6	2
norbornene	0.25	98	50	2.0	2
t-$BuCH{=}CH_2$	2	69	35	1.1	2

concentrations, where the conditions permitted loss of olefin in the oxygen stream. When benzene was the solvent, the yield of phenyl benzoate was between 29 and 45%, with biphenyl in approximately 5% yield.

Table I shows the results of VPC analyses of a series of benzil-sensitized photoepoxidations in benzene as solvent. Table II gives the corrected results in benzene for epoxidations of five olefins previously reported.[3]

There is an extreme variation of about twofold in the epoxide yields from norbornene in benzene over a range of concentrations in our two laboratories. The experimental condition most difficult to standardize is the light source; in a series of experiments[1] in methylene chloride, the light source was varied from a projection lamp (48 h, (epoxide)/(benzil consumed) = 0.42) to a 450-W Hanovia arc with a Corning 3387 filter, λ_{max} 436–466 nm (5.25 h, (epoxide)/(benzil consumed) = 1.11). Irradiation with the latter lamp with a potassium chromate filter, λ_{max} 313 nm, for 0.75 h consumed 10.6% of the benzil but yielded no epoxide.

Experimental Section

The irradiations in benzene were carried out at temperatures between 7 and 10 °C, with oxygen being constantly bubbled through the solution. Vapor chromatography was carried out with hexadecane[1] or diphenylmethane[2] as internal standard on a 5-ft 5% SE-30 column[1] or a 1-m 25% SE-30 column on Chromosorb W 60–80 mesh).[2] The light source was a Hanovia[1] or Eiko-sha[2] 450-W lamp in a Pyrex jacket.

In addition to the products mentioned above, the norbornene epoxidations[2] yielded about 4% of a product with longer retention time than benzil and with IR and ^1H NMR spectra suggesting a norbornanediol monobenzoate: IR (neat) 3470 (br), 1720, 1705, 1205, 1110, 780, 750, 700 cm^{-1}; ^1H NMR (CCl_4) δ 0.8–2.7 (br m), 3.7–4.8 (br m), 7.0–7.6 (m), 7.7–8.2 (m); ratio ca. 5:1:1.5:1.

Conclusions

The present results confirm[4] that no chain character is inherent in the benzil-sensitized epoxidation reaction. However, a number of facts about this and related processes bear witness to the occurrence of competing reactions: the self-sensitized photoepoxidation of methoxymethylenefluorene,[5] the frequent competition of epoxidation with singlet oxygen reactions, and the general capability of benzophenone as an epoxidation sensitizer. Most of these competing processes are not understood, and they cannot be accounted for as incidental to a simple epoxidation by benzoylperoxy radicals. The authors concerned[3] deeply regret having made an erroneous report in this field, and efforts are being continued to arrive at a comprehensive view of the process.

Acknowledgment. We thank the Robert A. Welch Foundation and the National Science Foundation for support.

Registry No. Norbornene, 498-66-8; benzil, 134-81-6; $Ph_2C{=}CMe_2$, 781-33-9; *trans*-PhCH=CHMe, 873-66-5; *cis*-PhCH=CHMe, 766-90-5; *t*-$BuCH{=}CH_2$, 558-37-2.

---

(4) Sawaki, Y.; Ogata, Y. *J. Am. Chem. Soc.* **1981**, *103*, 2049.

(5) Bartlett, P. D.; Landis, M. E. *J. Am. Chem. Soc.* **1977**, *99*, 3033.

Reactivities of Norbornene-Type Double Bonds in Propellane Derivatives and Their Precursors; Furan as a Diene

Paul D. Bartlett,* Gerald L. Combs, Jr., Ai-Xuan Thi Le, William H. Watson,*[1] Jean Galloy,[1] and Michio Kimura[1]

Contribution from the Department of Chemistry, Texas Christian University, Fort Worth, Texas 76129. *Received November 9, 1981*

Abstract: Some of the factors determining reactivity of a norbornenic double bond have been investigated by measuring the rates of epoxidation of the syn and anti adducts (**3** and **4**) of cyclopentadiene to norbornene-2,3-dicarboxylic anhydride, the syn adduct **10** of furan to the same dienophile, and the anti adduct **5** of cyclopentadiene to norbornadiene-2,3-dicarboxylic anhydride. In this series the major determinant of double-bond reactivity is proximity in space to the anhydride group. Structures of the monounsaturated syn and anti adducts **10** and **15**, the anti cyclopentadiene adduct **4**, and its epoxide **6** have been determined by X-ray crystallography. In additions to dienophiles **1** and **2**, the use of furan rather than cyclopentadiene strongly favors the exo Alder's rule products **13** and **10**.

The effect of bicyclic ring structures, notably that of norbornene, on the reactivity of the double bond has been of interest for some time.[2] In this rigid system the angle strain and positions in space of neighboring groups can be precisely specified and correlations sought with the observed rates of reaction.[3] In a growing number of systems,[4-13] it has appeared that interactions between the π orbital of the double bond and the σ or n orbitals of neighboring

---

(1) Fastbios Laboratory, Department of Chemistry, Texas Christian University.

(2) Alder, K.; Flock, F. H.; Janssen, P. *Chem. Ber.* **1956**, *89*, 2689.

(3) Edman, J. R.; Simmons, H. E. *J. Org. Chem.* **1968**, *33*, 3808.

(4) Fukui, K.; Inagaki, S. *Chem. Lett.* **1974**, 509.

(5) Inagaki, S.; Fujimoto, H.; Fukui, K. *J. Am. Chem. Soc.* **1976**, *98*, 4054.

(6) Paquette, L. A.; Hertel, L. W.; Gleiter, R.; Böhm, M. C. *J. Am. Chem. Soc.* **1978**, *100*, 6510.

(7) Paquette, L. A.; Carr, R. V. C.; Böhm, M. C.; Gleiter, R. *J. Am. Chem. Soc.* **1980**, *102*, 1186.

(8) Böhm, M. C.; Carr, R. V. C.; Gleiter, R.; Paquette, L. A. *J. Am. Chem. Soc.* **1980**, *102*, 7218; **1981**, *103*, 2910.

0002-7863/82/1504-3131$01.25/0 © 1982 American Chemical Society

Chart I

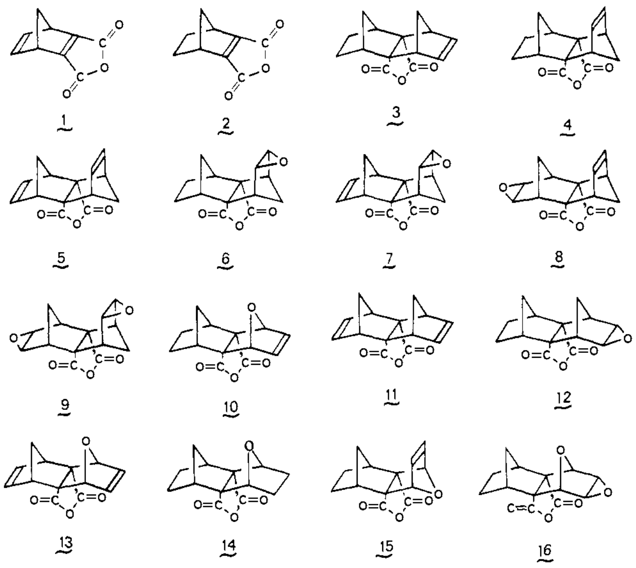

atoms may account for specific endo or exo directive effects as well as general reactivity and, in some cases, special geometry of the double bond.

The first synthesis of *anti*-sesquinorbornene[14] and also previous work beginning with a similar synthesis[3] involved some striking stereoselectivities in Diels–Alder reactions leading predominantly to the propellanes **3**–**5** and **11**, and some very tight classical steric hindrance in the *syn*-propellane anhydrides (**3** and its hydrogenation product) (see Chart I).

Specifically, in the addition of cyclopentadiene to norbornene-2,3-dicarboxylic anhydride (**2**), comparable amounts of the Alder's rule and anti-Alder's rule adducts **3** and **4** were obtained,[14] representing an increase in the Alder/anti-Alder product ratio of over 40-fold compared to the reaction with the doubly unsaturated anhydride **1**.[3] These results were independent of whether alumina was used to catalyze the addition,[14] and no time dependencies of the product ratio were observed.

We have now found that the use of furan instead of cyclopentadiene leads to a 20;1 ratio of the Alder's rule product **10** to the anti-Alder's rule product **15** from anhydride **2**. In the case of the doubly unsaturated anhydride **1**, furan added to yield the Alder's rule product **13** in high yield with no detectable presence of a second isomer. Toward the typical dienophile maleic anhydride, furan has been observed not only to be a less reactive diene than cyclopentadiene but also to yield Alder's rule products reversibly, which during prolonged reaction are converted into the more thermodynamically stable exo isomers.[20] In the present instance no reversibility could be detected in the formation of either **10** or **13**. It would appear that Alder's rule is not dominant (either positively or negatively) in determining the *thermodynamic* stability of the product, a more important factor here being the interaction between the CH_2 and O bridges, which could operate similarly in transition state and product.

The structures of **10** and **15** were determined by X-ray crystallography; that of **13** was established by the fact that it and **10** were quantitatively hydrogenated to the same saturated anhydride **14**.

The forces which operate in Alder's rule are the initial donor–acceptor interactions between the π systems of diene and dienophile, both π systems being normally coplanar. As the immediate sequel to this interaction, σ bonding develops, this process being rapid enough so that the Diels–Alder reaction is classified as having an early transition state,[23] with no energy minimum corresponding to an initial π complex. In the addition of cyclopentadiene to anhydride **1** or **2** the initial approach geometry must be displaced from the ideal Alder parallel-plane configuration by the spatial conflict between the CH_2 of the cyclopentadiene and the methylene bridge of the dienophile. The feasibility of a smooth Alder addition thus depends on (a) the possible resolution of this hindrance in the new geometry of the product and (b) the existence of a reaction path in which the initial and final bonding forces can merge into each other without being too much weakened by the steric forces at an intermediate stage.

It is obvious that the relative rates of Alder and anti-Alder additions in the present system depend critically on the balance of these forces. As far as the difference between cyclopentadiene and furan is concerned, the repulsive interaction beween CH_2 and CH_2 in the Alder transition state may well be replaced by a mildly attractive interaction between CH_2 and the O of furan. This interaction, which must begin in the orientation of the initial approach, is still evident in the dimensions of the final product: a less-than-favorable H_9–H_{10} distance of 1.80 Å in **3**, and a corresponding H–O distance in **10** of 2.20 Å, which might well represent more of an energy minimum.

The difference between dienophiles **1** and **2** may be more complicated, since the remote double bond favors anti-Alder addition of cyclopentadiene but Alder addition of furan. If we are near the critical energies for these two modes of addition, it could well be that a small additional force displacing the methylene bridge of **1** toward the anhydride group might have this effect, destabilizing the Alder's rule transition state for cyclopentadiene but stabilizing it for furan. Forces have been noted in recent studies of *syn*-sesquinorbornene[10,21] that might cause the remote double bond to exert a force in this direction.

In *endo*-1,4-*exo*-5,8-dimethano-*cis*-1,4,4a,5,6,7,8,8a-octahydronaphthalene, the parent hydrocarbon of **4**, the reactivity of the 2,3 double bond as affected by substituents on the neighboring methylene bridge has been the subject of careful study.[24] The rate of peracid epoxidation was increased 13-fold by a *cis*-methoxy group on the neighboring bridge, and decreased 25-fold when the bridge group was carbonyl instead of methylene. Similar effects were observed on (2 + 4) cycloadditions. In these norbornenic systems, the epoxidation always occurred on the exo face of the double bond. However, in [4.4.3]propellenes, with unbridged rings, the steric forces are sufficiently balanced so that, depending on the substituents on the five-membered ring, epoxidation occurs on both faces of the double bond.[25]

We undertook to compare the reactivities of the double bonds in the series **3**, **4**, **5**, **7**, **8** and **10** toward *m*-chloroperbenzoic acid (MCPBA) as a measure of the effect of including the anhydride

---

(9) Huisgen, R.; Ooms, P. H. J.; Mingin, M.; Allinger, N. L. *J. Am. Chem. Soc.* **1980**, *102*, 395.

(10) Watson, W. H.; Galloy, J.; Bartlett, P. D.; Roof, A. A. M. *J. Am. Chem. Soc.* **1981**, *103*, 2022.

(11) Avenati, M.; Hagenbuch, J.-P.; Mahaim, C.; Vogel, P. *Tetrahedron Lett.* **1980**, *21*, 3167.

(12) Pinkerton, A. A.; Schwarzenbach, D.; Stibbard, J. H. A.; Carrupt, P. A.; Vogel, P. *J. Am. Chem. Soc.* **1981**, *103*, 2095.

(13) Wagner, H.-U.; Szeimies, G.; Chandrasekhar, J.; Schleyer, P. V. R.; Pople, J. A.; Bimkley, J. J. *J. Am. Chem. Soc.* **1978**, *100*, 1210.

(14) Bartlett, P. D.; Blakeney, A. J.; Kimura, M.; Watson, W. H. *J. Am. Chem. Soc.* **1980**, *102*, 1383.

(15) Padwa, A.; Brodsky, L. *Tetrahedron Lett.* **1973**, 1045.

(16) Jefford, C. W; Boschung, A. F.; Rimbault, C. G. *Helv. Chim. Acta* **1976**, *59*, 2542.

(17) Johnson, C. K. ORTEP II. Report ORNL-3794, revised. Oak Ridge National Laboratory, TN, 1971.

(18) Main, P.; Lessinger, L.; Woolfson, M. M.; Germain, G.; Declercq, J. P. MULTAN78 "A System of Computer Programs for the Automatic Solution of Crystal Structures from X-ray Diffraction Data"; University of York: York, England; and University of Louvain: Louvain, Belgium, 1978.

(19) Stewart, J. M.; Machin, P. A.; Dickinson, C. W.; Ammon, H. L.; Flack, H.; Heck, H. "The XRAY76 System". Computer Science Center, University of Maryland, College Park, MD, 1976, Technical Report TR-446.

(20) Lee, M. W.; Herndon, W. C. *J. Org. Chem.* **1978**, *43*, 518.

(21) Bartlett, P. D.; Roof, A. A. M.; Winter, W. J. *J. Am. Chem. Soc.* **1981**, *103*, 6520.

(22) Larson, A. C. "Crystallographic Computing"; Ahmed, F. R., Hall, S. R., Huber, C. P., Eds.; Munksgaard: Copenhagen, 1970; pp 291–294.

(23) Huisgen, R. *Pure Appl. Chem.* **1981**, *53*, 171.

(24) Paddon-Row, M. N.; Patney, H. K.; Warrener, R. N. *Chem. Commun.* **1978**, 296.

(25) Mayer, W. J. W.; Oren, I.; Ginsburg, D. *Tetrahedron* **1976**, *32*, 1005.

Table I. Reactivities of Norbornenic Double Bonds toward *m*-Chloroperbenzoic Acid

compound	10^5k, M^{-1} s^{-1}	relative *k*
3	3.6	1.0
4	68	19
5 (double bond syn to anhydride)	4.2	1.2
5 (double bond anti to anhydride)	37.5	9
7	1.4	0.4
8	30	8.3
10	2.1	0.58

ring in the system. For the purpose of comparisons of reactivity, rate studies were made under the same experimental conditions for **3**, **4**, **5**, and **10**. Solutions 0.02 M in both the olefin and MCPBA in methylene chloride were prepared by dissolving at 0 °C and warmed to 25 °C, and samples were taken over periods of 50–100 h. The ratio of epoxide to unreacted hydrocarbon was determined by quenching the aliquots with 10% sodium bisulfite solution and analyzing by vapor phase chromatography with hexadecane as internal standard. Authentic samples of the epoxides **6**, **7**, **9**, **12**, and **16** were prepared and characterized as described in the Experimental Section. Due to difficulties in isolating a pure sample of epoxide **8**, this compound was characterized solely by its mass spectrum, which was identical in many respects with that of the isomeric epoxide **7**. Also it was found that upon further treatment of a mixture of **7** and **8** with MCPBA, these were converted completely to the diepoxide **9**. A clear distinction between the structures of isomeric **7** and **8** was possible when it was found that upon hydrogenation, **7** could be converted quantitatively to **6**.

Conveniently, when the reactants are at equal concentrations, the fraction (e/xx_0) is equal to kt, where e = [epoxide], x = [olefin] at time t, and x_0 = initial olefin concentration. Plots of this fraction against time for the four propellanes **3**, **4**, **5**, and **10** were linear over the entire time interval, with correlation coefficients of 0.995–0.999, leading to the bimolecular rate constants listed in Table I.

Both double bonds of **5** react simultaneously, but the product analysis indicates that the reaction of one of them predominates over the other by a factor of about 9. This accounts for the fact that, over the 60% reaction of **5** observed, the small departure from the 1:1 ratio of consumption of reactants does not cause an appreciable deviation from linearity of the plot.

The epoxide **6** was apparently a minor contaminant in the olefin **4**. As with other mildly strained olefins,[15,16] propellanes **3**, **4**, and **5** could all be epoxidized by molecular oxygen initiated by azobis(isobutyronitrile) (AIBN), but the uninitiated rate was too low for convenient measurement. Nevertheless, there was evidence that the sample of **5** used in the kinetic study, in the course of recrystallization, had undergone some conversion to the epoxide **7**: the concentrations of **5** extrapolated not to the intended initial 0.0248 M but to 0.0189 M. The missing 0.0059 M, if assumed to be **7**, fitted smoothly on the curve of its concentrations determined by vapor chromatography. These corrected initial concentrations were taken into account in the calculations leading to the assignment of the four rate constants involved in this system.

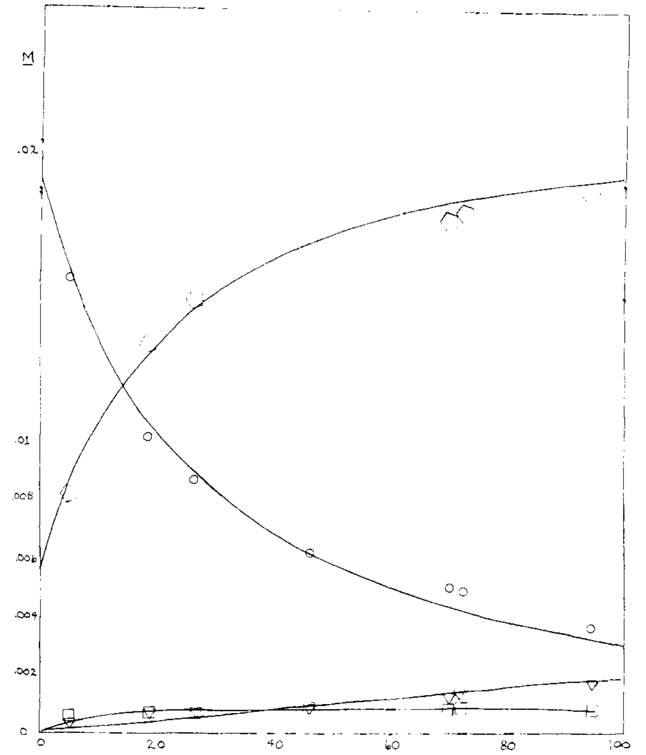

Figure 1. Calculated and observed concentrations of **5**, 7, **8**, and **9** in the epoxidation run of Table II. Observed values: **5**, circles; 7, pentagons; **8**, squares; **9**, triangles. Lines are calculated values assuming the initial concentrations and rate constants of Table II, footnote *a*.

For estimates of the four rate constants actually involved in the reaction of MCPBA with **5**, a series of aliquots were taken and analyzed with respect to the three epoxides **7**, **8**, and **9**, as well as the starting hydrocarbon. It is seen from Figure 1 that the slowly forming epoxide **8**, having a relatively reactive double bond, reaches a steady-state concentration after 46 h, at about 70% reaction, while the other epoxides continue to increase slowly throughout the period of observation. The data from these analyses allowed a set of successive approximations to the values of the rate constants, which were tested by incremental calculations on a computer; the values of time and concentrations of **5**, **7**, **8**, and **9** were calculated from the differential rate equations for 148 successive points along the reaction course, the assumed values of the rate constants being adjusted on the basis of the fit of each run to the experimental values of these concentrations. The selected values of the rate constants are shown in Table II, and the incrementally calculated concentrations are shown by the curves in Figure 1 and compared with the analytical values.

A test calculation showed that the course of a model second-order reaction with x_0 = 0.0189 M and k = 1.35 M^{-1} h^{-1} could

Table II. Stepwise Epoxidation of 5 by MCPBA

	5, M		7, M		8, M		9, M	
t,	calcd[a]	obsd[b]	calcd[a]	obsd[b]	calcd[a]	obsd[b]	calcd[a]	obsd[b]
1	0.0182	0.0216	0.0065	0.0030	0.0001	0.0003		
2	0.0176	0.0177	0.0071	0.0063	0.0001	0.0004		0.0003
3	0.0170	0.0178	0.0076	0.0062	0.0002	0.0005		0.0003
5	0.0159	0.0157	0.0086	0.0082	0.0003	0.0005	0.0001	0.0003
18.5	0.0108	0.0102	0.0130	0.0134	0.0007	0.0006	0.0003	0.0006
26.5	0.0090	0.0087	0.0146	0.0149	0.0007	0.0006	0.0005	0.0006
46	0.0062	0.0061	0.0169	0.0171	0.0008	0.0008	0.0009	0.0008
70	0.0043	0.0050	0.0184	0.0178	0.0008	0.0007	0.0013	0.0012
72.5	0.0042	0.0048	0.0185	0.0180	0.0008	0.0007	0.0014	0.0013
94.5	0.0032	0.0036	0.0192	0.0187	0.0007	0.0008	0.0017	0.0017

[a] Incremental calculation assuming [**5**] = 0.0189, [**7**] = 0.0059, and [MCPBA] = 0.0248 at $t = 0$; $k_{5\to7} = 3.75 \times 10^{-4}$; $k_{5\to8} = 4.17 \times 10^{-5}$; $k_7 = 1.39 \times 10^{-5}$; $k_8 = 3.0 \times 10^{-4}$ M^{-1} s^{-1}. [b] By vapor phase chromatography.

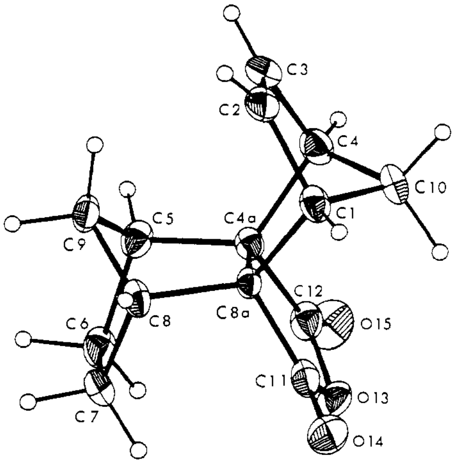

Figure 2. ORTEP drawing of compound **4**. The ellipsoids are drawn at the 35% probability level while the hydrogen atoms are represented by spheres of arbitrary size.

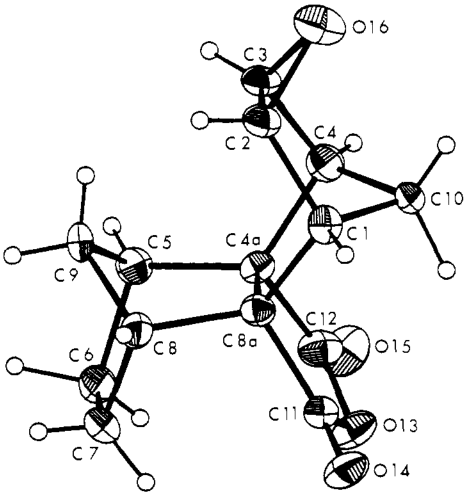

Figure 3. Drawing of compound 6. The ellipsoids are drawn at the 35% probability level while the hydrogen atoms are represented by spheres of arbitrary size.

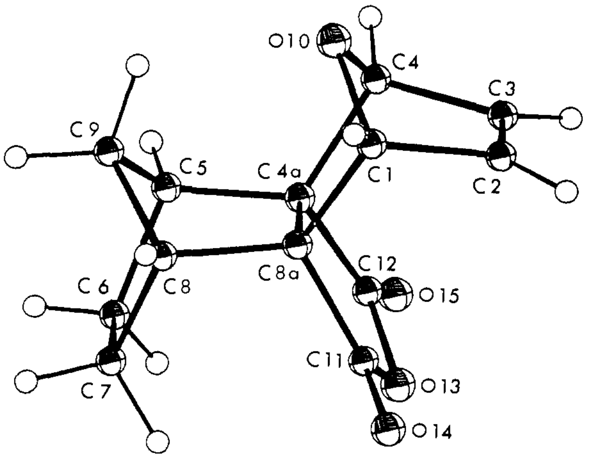

Figure 4. ORTEP drawing of compound **10**. The ellipsoids are drawn at the 35% probability level while the hydrogen atoms are represented by spheres of arbitrary size.

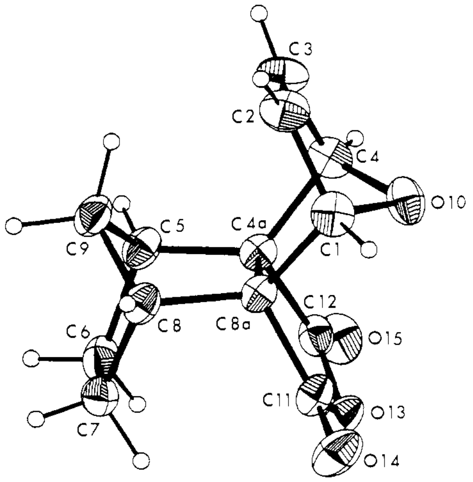

Figure 5. ORTEP drawing of compound **15**. The ellipsoids are drawn at the 35% probability level while hydrogen atoms are represented by spheres of arbitrary size.

be calculated incrementally with 160 points over 84% of its course, matching the concentrations from the integrated rate equation within a maximum error of 0.00005 M, or 0.26% of x_0.

It can be seen from Table I that of the seven double bonds whose reactivities were observed, those syn to an anhydride group showed epoxidation rate constants between 1.4 and 4.2 × 10^{-5} M^{-1} s^{-1}, while the double bonds syn to a methylene bridge were an order of magnitude more reactive, with *k*'s of (30–68) × 10^{-5}. As would be expected from the work of Paddon-Row et al.[24] the anhydride ring is the only important influence on the reactivity of these double bonds. The factor of 9–19 by which its presence depresses the epoxidation rate in anti structures is less than the factor of 25 previously observed for a carbonyl bridge,[24] a normal result of the anhydride oxygen atom delocalizing the charge on the carbonyl carbon atoms.

Figures 2, 3, 4, and 5 are ORTEP drawings[17] of compounds **4**, **6**, **10**, and **15**, while Tables III and IV present interatomic distances and valence angles. Figures 6 and 7 show important interplanar angles and intramolecular contacts. Although the hydrogen atom positions are not located accurately, the hydrogen atoms on C(2) and C(3) in compounds **3**,[14] **4**, **10**, and **15** appear to be bent away from the methylene and oxo bridges by 3°, 6°, 4°, and 1°, respectively. While any single observation might be questionable, the consistent bending of the hydrogen atoms away from the methylene or oxo bridge is significant.

The exclusive exo epoxidation observed here is consistent with steric hindrance to endo attack since H(9en)–C(2,3) = 2.48 Å and 2.43 Å in **4** and **15** while C(2,3)–C(11,12) = 2.77 Å and 2.72 Å in **10** and **3**. The central interplanar angle is 129.3° in **15**, 128.4° in **4**, 125.7° in **3**, and 122.7° in **10**. The closest approaches to H(9en) for the three compounds are H(9en)–H(10en) = 1.80 Å in **3**, H(9en)–O(10) = 2.20 Å in **10**, and the distance from H(9en) to the center of the C(2)–C(3) double bond of 2.34 Å in **15** and 2.40 Å in **4**. The reduction in the central interplanar angle upon going from **3** to **10** is readily understood; however, the larger angle in **4** and **15** may result from H(9en)–π-cloud repulsion or reduced repulsion between the anhydride and the methylene or oxo bridges.

The exo faces of the double bonds are sterically accessible and the greater reactivity of **4** and **15** compared to **3** and **10** must be attributed to other factors. The carbon atoms C(11) and C(12) lie an average of 2.72 and 2.77 Å from the carbon atoms C(2) and C(3) in **3** and **10**. The close proximity and suitable orientation of orbitals ensures significant overlap of the π system and together with partial positive charges on the carbonyl carbon atoms must lead to significant orbital modification. The nature of the π system in which the double bond is syn to the anhydride differs significantly from the isolated ethylenic π system in compounds where the methylene is anti to the anhydride. A series of low-temperature X-ray and neutron diffraction experiments has been initiated to investigate π-electron distributions and the accurate location of hydrogen atom positions.

Experimental Section

Preparations. Dimethyl acetylenedicarboxylate, furan, dicyclopentadiene, and *m*-chloroperbenzoic acid were obtained from Aldrich Chemical Co. Ethoxyacetylene was obtained from Pfaltz and Bauer.

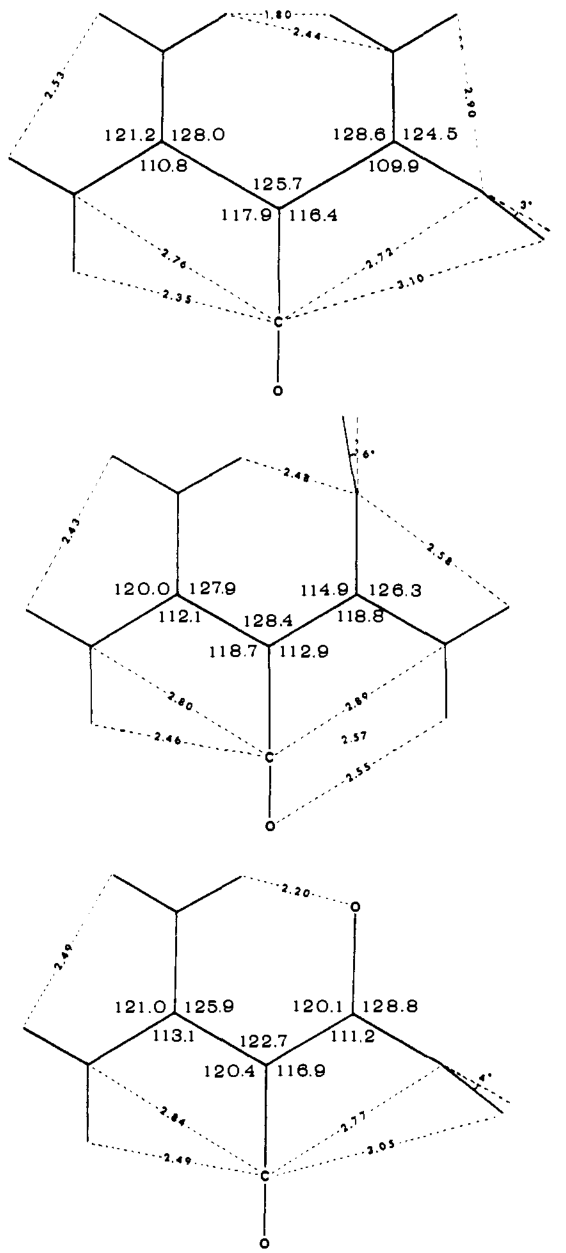

Figure 6. Important interplanar angles (deg) and intramolecular contacts (Å) for compounds 3[14] (top), 4 (middle), and 10 (bottom).

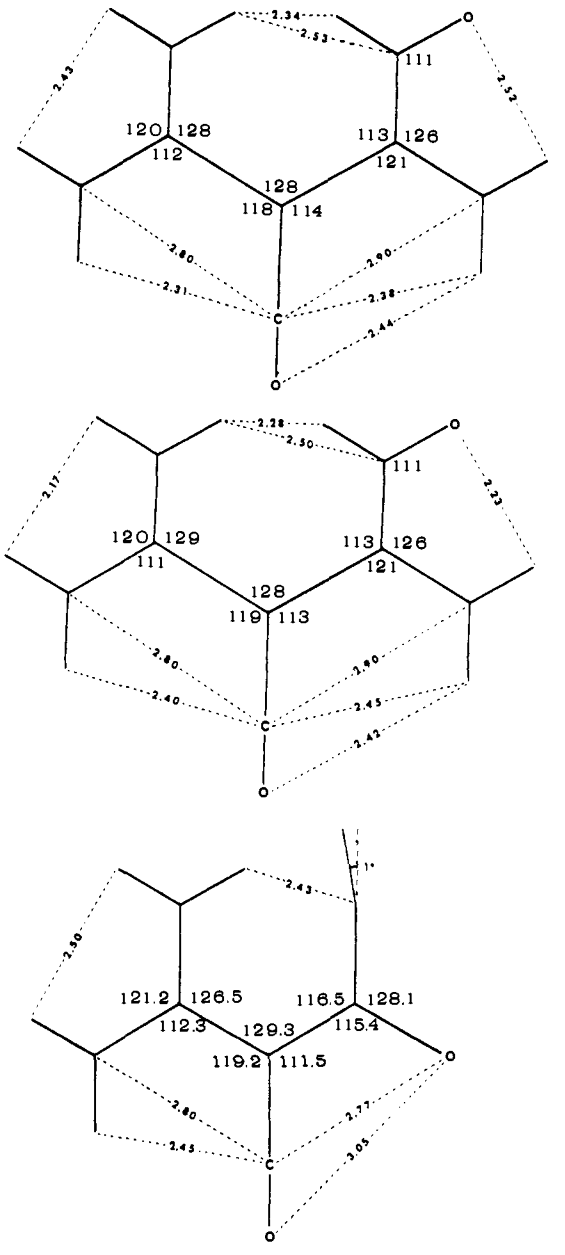

Figure 7. Important interplanar angles (deg) and intramolecular contacts (Å) for the two independent molecules of 6 and 15 (bottom).

The solvents were spectral grade from Aldrich Chemical Co. The silica gel used in the Diels–Alder reactions was 60 Pf-254 for preparative chromatography by EM reagents and obtained from Brinkmann. The silica gel used for column chromatography separations was 60–200 mesh obtained from Baker Chemical Co. The neutral aluminum oxide used in isomer separation was activity grade 1 manufactured for ICN Nutritional Biochemicals by Woelm Pharma. Benzene was distilled over sodium. Cyclopentadiene was from freshly cracked dicyclopentadiene. Mass spectra were obtained with a Finnigan OWA-1020 GC-MS-DS. NMR spectra were obtained with JEOL-FX60 and Varian EM-390 NMR spectrometers in $CDCl_3$ with internal Me_4Si as reference unless otherwise noted. Gas chromatographic analyses during kinetic reactions were done on a Perkin-Elmer Sigma 3 gas chromatograph apparatus with a 6-ft 5% SE-30 column. IR spectra were taken on a Perkin-Elmer 197 infrared spectrophotometer. Melting points were uncorrected and were taken on a Hoover capillary melting point apparatus. The anhydrides **1**, **5**, and **11** were prepared according to the previously described method of Edman and Simmons.[3] Anhydrides **2**, **3**, and **4** were prepared according to Bartlett, Blakeney, Kumura, and Watson.[14]

1,2,3,4,4a,5,8,8a-Octahydro-5,8-*exo*-oxa-1,4-*exo*-methanonaphthalene-4a,8a-dicarboxylic Anhydride (10) and 1,2,3,4,4a,5,8,8a-Octahydro-5,8-*endo*-oxa-1,4-*exo*-methanonaphthalene-4a,8a-dicarboxylic Anhydride (15). Norbornene-2,3-dicarboxylic anhydride (**2**) (7.94 g, 48 mmol) was dissolved in 100 mL of furan (95 g, 1.40 mol) and the solution stirred under nitrogen for 24 h at room temperature. The excess furan was removed (rotavap) and the resulting yellow solid was chromatographed repeatedly on a silica gel column, followed by thin-layer chromatography on silica gel, methylene chloride being the eluent in both cases. Chromatography separated **10** and **15** in relative amounts of 20:1.

10 is a white solid: mp 146–147 °C; ^1H NMR δ 6.42 (br s, 2 H), 4.98 (br s, 2 H), 2.76 (br s, 2 H), 1.8–1.2 (m, 6 H); ^{13}C NMR δ 170.55, 137.42, 82.71, 67.18, 41.52, 39.57, 26.44; IR (KBr disk) 1857 and 1777 cm^{-1}.

15 is a white solid: mp 145–146 °C; ^1H NMR δ 6.50 (br s, 2 H), 5.23 (br s, 2 H), 2.52 (br s, 2 H), 1.8–1.1 (m, 6 H); ^{13}C NMR δ 173.22, 137.36, 84.08, 67.44, 38.40, 37.88, 27.68; IR (KBr disk) 1853, 1775 cm^{-1}.

In another preparation, heated under reflux for 18 h, the combined yield of **10** and **15** was 96%.

1,4,4a,5,8,8a-Hexahydro-1,4-*exo*-oxa-5,8-*exo*-methanonaphthalene-4a,8a-dicarboxylic Anhydride (13). Norbornadiene-2,3-dicarboxylic anhydride (**1**) (100 mg, 0.62 mmol) was dissolved in furan (5 mL, 70 mmol) and stirred under nitrogen for 18 h, and the excess furan removed. The ^1H and ^{13}C NMR spectra of the crude product revealed the formation of a single isomer with no clear evidence of a second isomer. **13** is a white solid that can be recrystallized from ether: yield 97%; mp 148.5–150 °C; ^1H NMR δ 6.67 (br s, 2H), 6.43 (br s, 2 H), 5.03 (br s, 2 H), 3.27 (br s, 2 H), 3.03 (d, 1 H, $J = 9$ Hz), 1.77 (d, 1 H, $J = 9$ Hz); ^{13}C NMR δ 170.36, 141.38, 139.89, 81.80, 72.19, 49.57, 46.78; IR (KBr disk) 1859, 1759 cm^{-1}.

Table III. Interatomic Distances[a] (Å) for 4, 6, 10, and 15

	4	**10**	**15**	6_1	6_2
C(1)–C(8a)	1.577 (9)	1.577 (6)	1.548 (6)	1.56 (1)	1.56 (1)
C(1)–C(2)	1.512 (8)	1.510 (7)	1.502 (7)	1.52 (2)	1.52 (1)
C(2)–C(3)	1.313 (7)	1.320 (5)	1.309 (8)	1.43 (1)	1.44 (1)
C(3)–C(4)	1.504 (8)	1.502 (7)	1.483 (7)	1.53 (1)	1.54 (1)
C(4)–C(4a)	1.585 (9)	1.581 (5)	1.555 (6)	1.60 (1)	1.56 (1)
C(4a)–C(5)	1.554 (9)	1.533 (6)	1.559 (6)	1.54 (1)	1.57 (1)
C(5)–C(6)	1.558 (10)	1.539 (7)	1.528 (6)	1.55 (1)	1.56 (2)
C(6)–C(7)	1.554 (8)	1.538 (5)	1.544 (8)	1.57 (1)	1.54 (2)
C(7)–C(8)	1.550 (9)	1.546 (7)	1.530 (7)	1.55 (1)	1.52 (1)
C(8)–C(8a)	1.546 (9)	1.542 (5)	1.550 (6)	1.57 (1)	1.57 (1)
C(4a)–C(8a)	1.544 (6)	1.533 (4)	1.540 (6)	1.56 (1)	1.58 (1)
C(5)–C(9)	1.540 (7)	1.545 (8)	1.526 (7)	1.56 (1)	1.52 (1)
C(8)–C(9)	1.544 (7)	1.537 (7)	1.539 (7)	1.54 (1)	1.54 (1)
C(1)–C/O(10)	1.548 (8)	1.429 (6)	1.448 (6)	1.54 (1)	1.56 (1)
C(4)–C/O(10)	1.557 (8)	1.433 (6)	1.451 (6)	1.57 (1)	1.56 (1)
C(2)–O(16)				1.45 (1)	1.44 (1)
C(3)–O(16)				1.44 (1)	1.44 (1)
C(8a)–C(11)	1.495 (7)	1.493 (8)	1.509 (5)	1.48 (1)	1.50 (1)
C(4a)–C(12)	1.505 (7)	1.495 (8)	1.493 (6)	1.48 (1)	1.49 (1)
C(11)–O(13)	1.391 (6)	1.394 (5)	1.394 (5)	1.42 (1)	1.39 (1)
C(12)–O(13)	1.410 (6)	1.385 (5)	1.391 (6)	1.42 (1)	1.40 (1)
C(11)–O(14)	1.194 (6)	1.182 (4)	1.187 (5)	1.22 (1)	1.17 (1)
C(12)–O(15)	1.186 (6)	1.187 (5)	1.186 (6)	1.20 (1)	1.20 (1)
C(2)–C(11)[b]		2.769 (6)			
C(7)–C(11)[b]	2.80 (1)	2.840 (6)	2.808 (7)	2.80 (2)	2.80 (1)
C(11)–H(7en)[b]	2.46 (7)	2.49 (3)	2.45 (4)	2.31 (9)	2.40 (9)
O(13)–H(7en)[b]	2.88 (6)	2.94 (4)	2.90 (4)	2.76 (9)	2.86 (10)
C(11)–H(10en)[b]	2.57 (6)			2.38 (9)	2.45 (6)
O(13)–H(10en)	2.55 (6)			2.44 (10)	2.42 (7)
C(2)–H(9en)[b]	2.48 (7)		2.43 (4)	2.53 (9)	2.50 (8)
H(2en)–H(9en)[b]				2.34 (12)	2.28 (11)
H(9en)–O(10)		2.20 (4)			
H(9ex)–H(6ex)[b]	2.43 (7)	2.49 (8)	2.50 (5)	2.43 (16)	2.17 (15)
H(10ex)–O(16)				2.52 (1)	2.23 (10)

[a] Average deviation shown in parentheses. [b] Equivalent values averaged.

1,2,3,4,4a,5,6,7,8,8a-Decahydro-1,4-*exo*-oxa-5,8-*exo*-methanonaphthalene-4a,8a-dicarboxylic Anhydride (14). Samples of **14** were prepared (a) by Pd/charcoal hydrogenation of **10** in a Parr shaker at 15 psi in ethyl acetate and (b) by hydrogenation of **13** with the same catalyst and apparatus at 20 psi in ethanol. Both samples of **14** had identical properties: ^{1}H NMR δ 4.58 (br s, 2 H), 2.95 (br d, 1 H), 2.68 (br s, 2 H), 1.88 (br s, 4 H), 1.8–1.2 (m, 5 H); ^{13}C NMR δ 171.59, 81.87, 71.54, 42.95, 40.09, 27.87, 26.51. **14** is a white solid (mp 161.5–163.5 °C) and has IR absorptions at 1852 and 1756 cm^{-1} (KBr disk).

Decahydro-2,3-*exo*-epoxy-1,4-*endo*-5,8-*exo*-dimethanonaphthalene-4a,8a-dicarboxylic Anhydride (6). **4** (0.15 g, 0.00065 mol) was stirred in 10 mL of CH_2Cl_2 at 0 °C. MCPBA (80%, 0.15 g, 0.00069 mol) in 5 mL of CH_2Cl_2 was added dropwise to the solution and the reaction flask was stirred at room temperature for 38 h. The solution was washed with sodium bisulfite (10%), 10% $NaHCO_3$, and H_2O. The organic layer was dried over $MgSO_4$, and the solvent was removed to give a white solid. The product was recrystallized from EtOH to give a white solid: yield 81%; mp 260–270 °C; ^{1}H NMR δ 3.27 (s, 2 H), 3.06 (s, 2 H), 2.75 (s, 2 H), 2.42 (d, 1 H, J = 10 Hz), 1.9–1.2 (m, 6 H), 0.75 (d, 1 H, J = 10 Hz); ^{13}C NMR δ 173.74, 66.66, 50.55, 45.03, 41.52, 39.83, 27.55, 25.60; IR (KBr disk) 1851, 1763, 1213 cm^{-1}.

Decahydro-2,3-*exo*-epoxy-1,4-*exo*-5,8-*exo*-dimethanonaphthalene-4a,8a-dicarboxylic Anhydride (12). MCPBA (80%, 0.47 g, 0.00218 mol) in 10 mL of CH_2Cl_2 was added dropwise to a stirred solution of 0.5 g (0.00217 mol) of **3** in 15 mL of CH_2Cl_2 at 0 °C. After 2 days of refluxing, the reaction mixture was cooled, washed with 10% sodium bisulfite, 10% $NaHCO_3$, and H_2O, and dried over $MgSO_4$. CH_2Cl_2 was evaporated to leave the crude product, which was then eluted through a silica gel column (petroleum ether–ether, 5:1) followed by recrystallization (petroleum ether–ether) to give clear needles: yield 79%; mp 198.5–200.5 °C; ^{1}H NMR δ 3.23 (s, 2 H), 2.85 (s, 2 H), 2.8–2.3 (m, 3 H), 2.2–1.3 (m, 7 H); ^{13}C NMR δ 172.89, 68.61, 48.67, 43.66, 42.69, 42.36, 41.52, 26.44; IR (KBr disk) 1849, 1770, 1237 cm^{-1}).

1,4,4a,5,6,7,8,8a-Octahydro-6,7-*exo*-epoxy-1,4-*exo*-5,8-*endo*-dimethanonaphthalene-4a,8a-dicarboxylic Anhydride (7) and 1,2,3,4,4a,5,8,8a-Octahydro-2,3-*exo*-epoxy-1,4-*exo*-5,8-*endo*-dimethanonaphthalene-4a,8a-dicarboxylic Anhydride (8). **5** (0.154 g, 6.7 mmol) was dissolved in 20 mL of CH_2Cl_2 and cooled to 0 °C while 0.145 g (6.7 mmol) of 80% MCPBA in 7 mL of CH_2Cl_2 was added dropwise to the stirred solution. The mixture was left stirring at room temperature. At 94% completion of the reaction, the products were found to be 20.3:1:2.3 of **7**:**8**:**9** by VPC. The mixture was then washed with 10% sodium bisulfite, 10% $NaHCO_3$, and H_2O and dried ($MgSO_4$), and the solvent was removed (rotavap). Analysis of the crude reaction mixture by GC-MS demonstrated the very close similarity of the epoxides **7** and **8**: mass spectra, *m/z*, **7** 244 (1), 226 (2.5), 172 (19), 143 (39), 128 (70.6), 115 (47), 105 (15.4), 91 (12.6), 66 (100); mass spectra, *m/z*, **8** 244 (3), 226 (1.1), 143 (8.6), 128 (27.3), 115 (18.7), 105 (4.8), 91 (10.5), 66 (100).

Repeated recrystallization of the crude product from acetone–ether–petroleum ether gave pure **7**, a white solid: mp 268–280 °C; ^{1}H NMR δ 6.43 (s, 2 H), 3.31 (s, 2 H), 3.23 (s, 2 H), 3.03 (s, 2 H), 2.55 (d, 1 H, J = 10 Hz), 1.9–1.5 (m, 2 H), 1.14 (d, 1 H, J = 10 Hz); ^{13}C NMR δ 173.09, 141.71, 67.44, 50.74, 50.48, 45.03, 43.08, 29.76; IR (KBr disk) 1850, 1771, 1222 cm^{-1}.

Further proof of the exact structure of **7** came by hydrogenation of **7** in a Parr shaker apparatus with 5% Pd/charcoal catalyst in EtOAc at 5 psi H_2. After filtration through Celite and removal of the solvent, the remaining white solid was found to be identical in all respects (^{13}C and ^{1}H NMR, mp) with a sample of **6**.

Decahydro-2,3-*exo*-6,7-*exo*-diepoxy-1,4-*exo*-5,8-*endo*-dimethanonaphthalene-4a,8a-dicarboxylic Anhydride (9). **5** (0.158 g, 6.7 mmol) was dissolved into ice-cold CH_2Cl_2 (9 mL). MCPBA (0.40 g of 80%) in 10 mL of CH_2Cl_2 was added to the solution. The mixture was then refluxed for 2 days, cooled, washed with 10% sodium bisulfite, 5% of $NaHCO_3$, and H_2O, and dried with $MgSO_4$. CH_2Cl_2 was removed in vacuo. The crude product was rinsed with cold chloroform and dried to give **9**, a white solid: mp 330–343 °C dec; ^{1}H NMR δ 3.26 (s, 2 H), 3.21 (s, 2 H), 3.04 (s, 2 H), 2.92 (s, 2 H), 1.66 (s, 2 H), 1.20 (s, 2 H); ^{13}C NMR δ 172.24j, 66.34, 49.64, 44.38, 40.54, 26.70, 25.92, 25.34; IR (KBr disk) 1852, 1770, 1225 cm^{-1}.

Decahydro-1,4-*exo*-oxa-2,3-*exo*-epoxy-5,8-*exo*-methanonaphthalene-4a,8a-dicarboxylic Anhydride (16). **10** (0.148 g, 6.4 mmol) was dissolved in 10 mL of CH_2Cl_2, and to this solution was added dropwise 0.145 g (6.7 mmol) of 80% MCPBA in 7 mL of CH_2Cl_2. The resulting solution was refluxed while being stirred for 5 days, cooled, washed with 10% sodium bisulfite, 5% $NaHCO_3$, and H_2O, and dried ($MgSO_4$), and the solvent was removed (rotavap). Recrystallization of the residue from acetone–ether–petroleum ether gave a white solid: mp 170–174 °C; yield 80%; ^{1}H NMR δ 4.57 (s, 2 H), 3.48 (s, 2 H), 2.73 (br s, 2 H), 1.8–1.0 (m, 6

Table IV. Valence Angles (Deg) for **4**, 6, **10**, and **15**

	4	**10**	**15**	6_1	6_2
C(8a)C(1)C(2)	109.0 (5)	106.5 (4)	111.5 (4)	107.8 (6)	108.4 (6)
C(1)C(2)C(3)	107.9 (5)	105.6 (4)	105.4 (4)	106.4 (7)	106.6 (6)
C(2)C(3)C(4)	108.5 (5)	106.3 (4)	106.7 (4)	106.4 (8)	105.4 (7)
C(3)C(4)C(4a)	108.3 (5)	107.0 (4)	111.7 (4)	106.9 (5)	107.3 (6)
C(4)C(4a)C(8a)	103.3 (4)	101.2 (3)	100.9 (3)	103.0 (5)	103.6 (5)
C(4a)C(8a)C(1)	102.7 (4)	101.1 (2)	101.2 (3)	103.7 (6)	102.8 (5)
C(8a)C(1)C/O(10)	99.4 (4)	100.7 (3)	98.2 (3)	100.6 (5)	100.2 (5)
C(2)C(1)C/O(10)	99.2 (4)	101.2 (3)	101.5 (4)	100.6 (7)	100.3 (6)
C(1)C/O(10)C(4)	93.2 (5)	97.1 (4)	94.9 (3)	94.9 (6)	94.2 (6)
C(3)C(4)C/O(10)	99.1 (4)	101.1 (3)	101.2 (4)	99.6 (6)	100.4 (5)
C(4a)C(4)C/O(10)	98.8 (4)	100.1 (2)	98.3 (3)	98.6 (7)	99.9 (7)
C(4a)C(5)C(6)	107.0 (4)	108.3 (4)	107.0 (3)	108.4 (7)	107.4 (8)
C(5)C(6)C(7)	103.8 (5)	104.0 (4)	103.6 (4)	103.5 (7)	102.4 (7)
C(6)C(7)C(8)	103.5 (5)	103.4 (3)	103.6 (4)	103.8 (7)	105.8 (10)
C(7)C(8)C(8a)	107.8 (4)	108.1 (4)	108.3 (3)	106.8 (6)	106.3 (6)
C(8)C(8a)C(4a)	103.5 (4)	103.8 (3)	103.5 (3)	103.7 (5)	103.8 (5)
C(8a)C(4a)C(5)	104.2 (4)	103.9 (3)	103.3 (3)	103.5 (5)	102.5 (5)
C(4a)C(5)C(9)	102.7 (4)	102.0 (3)	103.1 (3)	103.4 (5)	104.0 (5)
C(6)C(5)C(9)	98.5 (5)	99.4 (3)	99.6 (4)	98.4 (6)	97.8 (6)
C(5)C(9)C(8)	95.6 (4)	94.8 (5)	95.2 (3)	95.5 (7)	97.2 (7)
C(7)C(8)C(9)	99.0 (5)	99.5 (4)	99.5 (4)	98.6 (6)	97.9 (7)
C(8a)C(8)C(9)	103.1 (4)	102.1 (2)	102.1 (3)	103.2 (6)	102.7 (6)
C(4a)C(8a)C(11)	104.7 (4)	104.6 (4)	103.9 (3)	103.9 (5)	104.3 (5)
C(8a)C(11)O(13)	110.8 (4)	110.0 (3)	110.2 (3)	111.5 (7)	109.6 (7)
C(11)O(13)C(12)	110.1 (4)	110.5 (4)	110.5 (3)	109.0 (7)	112.1 (7)
O(13)C(12)C(4a)	110.0 (4)	110.2 (3)	110.4 (4)	110.2 (5)	109.9 (5)
C(12)C(4a)C(8a)	104.4 (4)	104.5 (3)	104.9 (3)	105.2 (6)	104.2 (6)
C(8a)C(11)O(14)	129.8 (5)	130.7 (4)	130.2 (4)	131.5 (6)	129.5 (6)
O(13)C(11)O(14)	119.5 (5)	119.3 (5)	119.6 (4)	117.0 (8)	120.9 (8)
C(4a)C(12)O(15)	131.2 (5)	130.4 (4)	130.5 (4)	131.7 (9)	130.3 (9)
O(13)C(12)O(15)	118.9 (5)	119.3 (5)	119.1 (4)	118.1 (8)	119.8 (9)
C(1)C(8a)C(11)	108.5 (5)	112.8 (4)	107.7 (3)	109.0 (6)	108.6 (6)
C(8)C(8a)C(11)	112.8 (5)	114.7 (3)	112.8 (3)	113.1 (6)	112.9 (6)
C(4)C(4a)C(12)	107.9 (5)	111.8 (3)	107.6 (3)	107.0 (5)	108.0 (6)
C(5)C(4a)C(12)	113.1 (5)	114.5 (4)	114.3 (3)	113.9 (6)	114.2 (6)
C(4)C(4a)C(5)	121.9 (4)	118.4 (4)	123.3 (3)	122.2 (7)	122.1 (7)
C(1)C(8a)C(8)	122.6 (4)	117.4 (4)	124.8 (3)	121.3 (5)	122.3 (6)
C(1)C(2)O(16)				116.0 (7)	116.4 (6)
C(3)C(2)O(16)				59.9 (6)	59.9 (5)
C(2)C(3)O(16)				60.5 (6)	60.0 (5)
C(4)C(3)O(16)				115.0 (7)	115.4 (6)
C(2)O(16)C(3)				59.6 (5)	60.1 (5)

H); ^{13}C NMR δ 169.90, 78.75, 71.28, 47.43, 42.75, 40.61, and 26.25; IR (KBr disk) 1855, 1771, 1232 cm^{-1}.

X-ray Analysis. All X-ray data were collected on a Syntex P2_1 diffractometer system with graphite-monochromated Cu Kα (λ = 1.54178 Å) or Mo Kα (λ = 0.71069 Å) radiation (in the case of **6**). Room-temperature lattice parameters were refined by a least-squares procedure utilizing 15 reflections whose angles were measured by a centering routine associated with the Syntex diffractometer. Intensity data were collected by the θ–2θ scanning technique, using a variable scan speed with a maximum 2θ of 115° for compound **4**, 120° for compounds **6** and **10**, and 130° for compound **15**. Periodically monitored reflections showed no significant changes in intensities. The data were corrected for Lorentz and polarization factors, but no absorption corrections were applied. The direct methods program MULTAN78[18] was used to solve all structures. The structures were refined by a full-matrix least-squares technique with anisotropic thermal parameters for the nonhydrogen atoms.

The refinements were terminated when the average shift was of the order of one-tenth of the average esd. The R factor is defined as $R = \sum||F_o| - |F_c||/\sum|F_o|$. The function minimized was $\sum\omega(|F_o| - |F_c|)^2$, where $\omega = 1/\sigma^2(F_o)$ or $1/[\sigma^2(F_o) + (0.01F_o)^2]$. Scattering factors were calculated by the XRAY76[19] program. Tables of atomic positional parameters, anisotropic thermal parameters, and observed and calculated structure factors are included in the supplementary material.

Compound 4. A crystal of dimensions 1.3 × 0.75 × 0.3 mm was used to collect all data. The unit cell is triclinic, and statistics and structure solution indicated space group $P\bar{1}$.

Crystal Data. $C_{14}H_{14}O_3$: M_r = 230.3, a = 7.164 (2) Å, b = 8.289 (2) Å, c = 10.145 (2) Å, α = 96.30 (2)°, β = 92.22 (2)°, γ = 111.90 (2)°, V = 553.5 (3) Å^3, Z = 2, d_C = 1.38 g cm^{-3}, μ = 7.99 cm^{-1}.

Of the 1491 independent reflections measured with Cu Kα radiation, 1291 had intensities greater than $3\sigma(I)$. Phases were calculated for the 282 $|E|$ values greater than 1.3, and the phase set with highest combined figure of merit yielded an E map that revealed the positions of all nonhydrogen atoms. Full-matrix least-squares refinement reduced the R factor to 0.131. All hydrogen atoms were located in a difference map and further least-squares refinement led to a final R of 0.084.

Compound 6. Crystals of the epoxide were of very poor quality. A crystal of dimensions 0.30 × 0.20 × 0.50 mm was used for all data collection. The unit cell is monoclinic and systematic absences were consistent with space group $P2_1/a$.

Crystal Data. $C_{14}H_{14}O_4$: M_r = 246.3, a = 14.578 (7) Å, b = 12.186 (4) Å, c = 14.599 (10) Å, β = 119.22 (4)°, V = 2263 (2) Å^3, Z = 8, d_c = 1.445 g cm^{-3}, μ = 8.89 cm^{-1}; two independent molecules per asymmetric unit.

Of the 3812 independent reflections measured with Mo Kα radiation, 2114 had intensities greater than $2\sigma(I)$. Phases were calculated for the 200 $|E|$ values greater than 1.4, and the phase set with the highest combined figure of merit revealed the positions of 34 nonhydrogen atoms. Alternate least-squares refinements and difference Fourier calculations led to the location of the remaining atoms of the two independent molecules. Full-matrix least-squares refinement led to a final R factor of 0.088.

Compound 10. The unit cell is monoclinic and systematic extinctions were consistent with space group $P2_1/c$.

Crystal Data. $C_{13}H_{12}O_4$: M_r = 232.2, a = 15.982 (8) Å, b = 7.564 (2) Å, c = 12.084 (4) Å, β = 134.44 (2)°, V = 1042.9 (6) Å^3, Z = 4, d_c = 1.48 g cm^{-3}, μ = 9.29 cm^{-1}.

Of the 1407 independent reflections measured, 1124 had intensities greater than $3\sigma(I)$. Phases were calculated for the 262 $|E|$ values greater than 1.30, and the phase set with the highest combined figure of merit yielded an E map that revealed the positions of all nonhydrogen atoms. Full-matrix least-squares refinment led to an R of 0.133. All hydrogen atom positions were located in a difference map. A total of 14 strong reflections were eliminated because of extinction. Further least-squares refinement led to a final R of 0.087.

Compound 15. A crystal of dimensions 0.30 × 0.22 × 0.17 mm was used for all data collection. The unit cell is monoclinic and systematic absences were consistent with space group $P2_1/c$.

Crystal Data. $C_{13}H_{12}O_4$: $M_r = 232.2$, $a = 11.472\ (2)$ Å, $b = 7.635\ (2)$ Å, $c = 12.260\ (1)$ Å, $\beta = 96.72\ (1)$, $V = 1066.4\ (4)$ Å^3, $Z = 4$, $d_c = 1.45$ g cm^{-3}, $\mu = 9.09$ cm^{-1}.

Of the 1773 independent reflections collected, 961 had intensities greater than $3\sigma(I)$. Phases were calculated for the 191 $|E|$ values greater than 1.20 and the phase set with highest combined figure of merit yielded an E map that revealed the positions of all nonhydrogen atoms. After anisotropic refinement, all hydrogen atoms were located in a difference map. An isotropic extinction correction[22] introduced in the last cycles of refinement refined to a value of $11.8\ (2) \times 10^{-3}$ and yielded a final R factor of 0.035.

Acknowledgment. We thank the Robert A. Welch Foundation, the National Science Foundation, and the National Institutes of Health for support of this work.

Registry No. 1, 17397-31-8; **2**, 19479-86-8; **3**, 73711-63-4; **4**, 73654-74-7; **5**, 17397-36-3; 6, 81495-66-1; 7, 81423-95-2; **8**, 81446-05-1; **9**, 81423-96-3; **10**, 81423-97-4; **12**, 81423-98-5; **13**, 81423-99-6; **14**, 81424-00-2; **15**, 81446-06-2; **16**, 81424-01-3.

Supplementary Material Available: Tables of atomic positional parameters, anisotropic thermal parameters, and observed and calculated structure factors (60 pages). Ordering information is given on any current masthead page.

---

o-Carboranylcarbene and *m*-Carboranylcarbene[1,2]

Sarangan L. Chari, Sheau-Hwa Chiang, and Maitland Jones, Jr.*

Contribution from the Department of Chemistry, Princeton University, Princeton, New Jersey 08544. *Received July 30, 1981*

Abstract: Addition of *o*- and *m*-carboranylcarbene to olefins takes place in a largely stereospecific fashion. In the addition to cis olefins, it is the anti isomer that predominates. Insertion into carbon-hydrogen bonds occurs with a secondary/primary selectivity ratio of 3.0. (Methyl-*o*-carboranyl)carbene behaves like tolylcarbene in intramolecular reactions. It yields vinyl-*o*-carborane and the carborane analogue of benzocyclobutene. (Methyl-*m*-carboranyl)carbene does not give vinyl-*m*-carborane.

If one were set the task of choosing the archetypal carbene, one might well settle on phenylcarbene.[3] Not only are the properties of both the addition and insertion reactions well worked out but also it is possible to generate the carbene from several sources. This is important because comparisons of properties of the intermediate formed from several sources allow identification of the common reaction species as the *carbene*. Thus in this case, but not all others, reactive nitrogen-containing intermediates derived from phenyldiazomethane can be eliminated.[4] We wondered if the stability conferred by a phenyl group upon an adjacent divalent carbon would be duplicated by a carborane. Would the effect of "two-dimensional" aromaticity be resembled by those of the "three-dimensional" or "super aromaticity" of the carboranes? In considering the possibilities we must examine steric, inductive, and resonance effects.[5]

The term "superaromatic" has been justified by a variety of MO treatments.[5,6] A system of 13 bonding MO's is nicely filled by the 26 electrons (6 from the two carbons, 20 from the 10 borons) involved in framework bonding. The predicted stability finds support in the ease of substitution reactions[5,7] and of course in the renowned stability of the icosahedral frame which routinely survives 400 °C, suffering at higher temperatures only rearrangement from the ortho isomer to the meta (ca. 500 °C, quantitative in a flowing system at 600 °C) followed by a less clean conversion to para (50% at >600 °C).[5,8] However, it is *not* clear that this thermodynamic stability is accompanied by stabilizing effects on attached positions, as clearly is the case in benzene and its derivatives. A study of arylcarboranes showed that although the two icosahedrons, and especially the ortho isomer, were highly electron withdrawing inductively, there was no substantial ground state "extension of electron delocalization by interaction with the aryl group".[9] Similarly, there is no strong case to be made that the analogue of naphthalene, in which one benzene ring is replaced by a carborane,[10] is more than a diene appended to the icosahedron. Only the NMR spectrum provides tenuous evidence of aromatic behavior. Even here the chemical shift of the diene protons is only 0.2-0.3 ppm downfield from that expected of a diene.[11] Of direct impact on our projected work was the finding of Hutton and Roth of the Bell Laboratories group, along with one of us, that EPR spectra of *o*-carboranylcarbene and a C-methylated derivative showed little delocalization of π-spin density.[12]

On first thought it might be expected that there would be enormous steric differences between the flat, six-atom frame benzene ring and the 12-atom frame, three-dimensional icosahedral carboranes. Not so. The 2.8-Å para C-C bond distance in benzene is increased by only a few tenths of 1 Å in the various "para" distances in *o*-, *m*-, and *p*-carboranes.[6] The size difference is not so great as one might imagine. Carboranes are the size of slightly elongated, rotating benzene rings. One possible indication that size differences will be of minor import is the observation that in the interaction of *o*-carboranyl alanine with chymotrypsin, the carboranyl group could bind with the "phenyl recognition site".[13]

---

* It gives us great pleasure to dedicate this paper to Professor William von Eggers Doering on the occasion of his 65th birthday.

[1] *o*-Carborane and *m*-carborane are 1,2-dicarba-*closo*-dodecaborane (12) and 1,7-dicarba-*closo*-dodecaborane (12), respectively.

[2] A portion of this work was previously communicated: Chari, S.; Agopian, G. K.; Jones, M., Jr. *J. Am. Chem. Soc.* **1979**, *101*, 6125. Other portions come from the Ph.D. Thesis of S.L.C., Princeton University, 1981.

[3] For a summary see: Jones, M., Jr., Moss R. A., Eds. "Carbenes"; Wiley: New York, 1973; Vol. I, pp 64-73.

[4] For cases in which excited diazo compounds may play a role see: Moss, R. A.; Jones, M., Jr. In "Reactive Intermediates"; Wiley: New York, 1981; Vol. 2, Chapter 3.

[5] (a) Grimes, R. N. "Carboranes", Academic Press: New York, 1970. (b) Onak, T. "Organoborane Chemistry"; Academic Press: New York, 1975. (c) Beall, H. In "Boron Hydride Chemistry"; Muetterties, E. L., Ed.; Academic Press: New York, 1975; Chapter 9.

[6] Bohn, R. K.; Bohn, M. D. *Inorg. Chem.* **1971**, *10*, 350.

[7] For examples see: Potenza, J. A.; Lipscomb, W. N. *Inorg. Chem.* **1966**, *5*, 1471, 1478, 1483 (*o*-carborane). Stanko, V. I.; Klimova, A. I.; Titova, N. S. *Zh. Obshch. Khim.* **1968**, *38*, 2817 (*m*-carborane).

[8] Papetti, S.; Obenland, C.; Heying, T. L. *Ind. Eng. Chem. Prod. Res. Dev.* **1966**, *5*, 334.

[9] Hawthorne, M. F.; Berry, T. E.; Wegner, P. A. *J. Am. Chem. Soc.* **1965**, *87*, 4746.

[10] Matteson, D. S.; Hota, N. K. *J. Am. Chem. Soc.* **1971**, *93*, 2893.

[11] Cooper, M. A.; Manatt, S. L. *J. Am. Chem. Soc.* **1969**, *91*, 6325; **1970**, *92*, 1605.

[12] Hutton, R. S.; Roth, H. D.; Chari, S. *J. Phys. Chem.* **1981**, *85*, 753.

0002-7863/82/1504-3138$01.25/0